

Laser control of magnonic topological phases in antiferromagnets

Kouki Nakata,¹ Se Kwon Kim,² and Shintaro Takayoshi^{3,4}

¹*Advanced Science Research Center, Japan Atomic Energy Agency, Tokai 319-1195, Japan*

²*Department of Physics and Astronomy, University of Missouri, Columbia, Missouri 65211, USA*

³*Max Planck Institute for the Physics of Complex Systems, Dresden 01187, Germany*

⁴*Department of Quantum Matter Physics, University of Geneva, Geneva 1211, Switzerland*

(Dated: July 18, 2019)

We study the laser control of magnon topological phases induced by the Aharonov-Casher effect in insulating antiferromagnets (AFs). Since the laser electric field can be considered as a time-periodic perturbation, we apply the Floquet theory and perform the inverse frequency expansion by focusing on the high frequency region. Using the obtained effective Floquet Hamiltonian, we study nonequilibrium magnon dynamics away from the adiabatic limit and its effect on topological phenomena. We show that a linearly polarized laser can generate helical edge magnon states and induce the magnonic spin Nernst effect, whereas a circularly polarized laser can generate chiral edge magnon states and induce the magnonic thermal Hall effect. In particular, in the latter, we find that the direction of the magnon chiral edge modes and the resulting thermal Hall effect can be controlled by the chirality of the circularly polarized laser through the change from the left-circular to the right-circular polarization. Our results thus provide a handle to control and design magnon topological properties in the insulating AF.

I. INTRODUCTION

The utilization of the quantized spin wave, magnons, plays an increasingly important role in spintronics, spawning its subfield, magnon-spintronics a.k.a. magnonics [1, 2]. The main subject in this field is the realization of rapid and efficient transmission of information through spins. For this purpose, antiferromagnets (AFs) [3–5] have an advantage over ferromagnets (FMs) [6–8] in that the dynamics is much faster in the former since the former energy scale arising from microscopic and quantum-mechanical spin exchange interactions is much larger than the latter energy scale governed by the macroscopic magnetic dipole interaction.

Another important viewpoint is the error-tolerance of communication, and topology is a useful tool to realize the states robust against impurities. In Ref. [9], a magnonic topological insulator (TI) is realized in the AF with the electric field gradient making use of the opposite magnon chirality [10–12] associated with the Néel magnetic order. This gradient field behaves as the gauge potential for magnons through the Aharonov-Casher (AC) effect [13] and forms the Landau level of magnons in the bulk. In particular, magnons with the opposite magnon chirality carrying a magnetic dipole moment $\sigma g \mu_B \mathbf{e}_z$ with $\sigma = \pm 1$, where μ_B is the Bohr magneton and g is the g -factor of the constituent spins, propagate along the edge of the sample in the opposite direction and thus the helical edge modes are realized in AFs, being in contrast to the chiral edge mode in FMs [14] characterized by the single magnon chirality. The spin transport properties in such AFs have a topological nature and cannot be disturbed by local perturbations. Thus the next task is to elucidate how to manipulate the topology in magnonic TIs.

A conventional way to change the physical state is tuning the control parameters of the system, e.g., tempera-

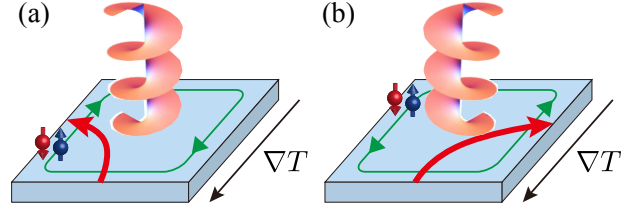


FIG. 1: Schematic representation of magnon states in two-dimensional AFs subjected to a laser. A circularly polarized laser (pink-colored spiral) generates a pair of chiral edge magnon states and induces magnonic thermal Hall effect where up and down magnons ($\sigma = \pm 1$ represented by blue and red balls with arrows, respectively) with opposite magnetic dipole moments $\sigma g \mu_B \mathbf{e}_z$ propagate along the edge of a finite size sample in the same direction. The direction of the magnon chiral edge modes (green lines with arrows) and the resulting thermal Hall current (red arrows) can be controlled by changing the chirality of the circularly polarized laser between the (a) right-circular $\eta = -1$ and (b) left-circular $\eta = 1$ polarization.

ture, pressure, and a static electromagnetic field. However a remarkable advance in the field of quantum optics offers a novel method to the manipulation of the state; the application of laser. A number of studies have been conducted both theoretically and experimentally on the laser-induced or -controlled states such as the photoinduced metal-insulator transition [15, 16], Floquet topological phases [17–21], and laser-induced magnetic states [22–26]. In particular, for magnetic systems, the typical energy scale is on the order of meV, which corresponds to the terahertz frequency. Thus spin manipulation is performed in the picosecond time interval and it is much faster than the time scale of conventional spintronics. Therefore establishing the way to control magnonic TIs [9] is an essential ingredient for the ultrafast topo-

logical magnonics.

In this paper, we consider the application of a laser to the insulating AF on the square lattice with an easy-axis magnetic anisotropy which hosts two kinds of gapped magnons with the same parabolic dispersion and the opposite magnetic dipole moment [9]. At low temperature [27], interaction effects such as magnon-magnon and magnon-phonon interactions become negligibly small [28–30]. We treat the effect of the laser as a time-periodic electric field, which is incorporated into the Hamiltonian as the time-periodic AC potential. This system can be analyzed by the Floquet theory and in the high frequency regime, we can obtain the effective Floquet Hamiltonian [19, 31] by the high frequency expansion. We find that the linearly polarized laser with nonzero time-averaged field induces helical magnon edge states, while the circularly polarized laser induces a pair of chiral magnon edge states (Fig. 1). The laser response depending on the direction of the magnetic dipole moment for each magnon plays an important role. In another perspective, our study corresponds to the further extension of Ref. [9] into the nonequilibrium regime away from the adiabatic limit. The resulting difference in the thermomagnetic properties [32–38] of Hall transport is also discussed.

This paper is organized as follows. In Sec. II, we quickly review the magnonic TI in the static situation. In Sec. III, considering three types of lasers, we derive each effective Floquet Hamiltonian and find the difference in the magnon motion focusing on the σ -dependence. The resulting difference in thermomagnetic properties of Hall transport is discussed in Sec. IV. In Sec. V, we provide a theoretical insight into experiments. Finally, we remark on several issues in Sec. VI and summarize in Sec. VII. Technical details are described in the Appendix.

II. MAGNONIC TI

Before considering the laser application, we quickly review the magnonic TI realized in the insulating AFs with the static electric field gradient. For the details, see Ref. [9]. The contents in this section are the basis for our study on the case of time-dependent electric field instead of the static field, which is discussed in the following sections.

It has been established that the spin-wave theory [39, 40] and its quantized version, the magnon picture [41], well describes the thermomagnetic properties such as magnetization and specific heat in the AFs [42, 43] as well as FMs. We consider the insulating AF on a two-dimensional square lattice residing in the xy plane with magnetic anisotropy that prefers the S^z axis. The ground state of this system has the Néel order along the z direction and the low energy excitation structure is dictated in terms of as electrically neutral bosonic quasiparticles after the Bogoliubov transformation. Here there exist two kinds of bosons carrying a magnetic dipole mo-

ment $\sigma g\mu_B \mathbf{e}_z$ with $\sigma \equiv \delta S^z = 1(-1)$, which are respectively identified with up (down) magnons. Due to the presence of easy-axis magnetic anisotropy, the insulating AFs have gapped and parabolic dispersion under the long wave-length approximation, and the dynamics can be described by using the decoupled two magnon modes ($\sigma = \pm 1$) at temperature lower than the magnon gap. In the low-energy regime, such an antiferromagnetic magnonic system effectively preserves the time-reversal symmetry (TRS).

In Ref. [9], under the assumption that the total spin along the z axis $\sum_j S_j^z$ is conserved and remains a good quantum number, we have proposed a magnonic analog of the quantum spin Hall effect characterized by helical edge states and thus established a bosonic counterpart of TIs [44, 45], namely the magnonic TIs in insulating AFs using the above-mentioned picture for the clean systems and following the work by Aharonov and Casher [13, 46]. The proposal is built upon the fact that an electric field couples to the magnetic dipole moment $\sigma g\mu_B \mathbf{e}_z$ through the AC effect [13, 47–55], which is analogous to the Aharonov-Bohm (AB) effect [56–58] of electrically charged particles in magnetic fields. Each magnon ($\sigma = \pm 1$) of the insulating AF subjected to a dc electric field with \mathcal{E} a constant gradient $\mathbf{E}(\mathbf{r}) = \mathcal{E}(-x, 0, 0)$ as a function of the position $\mathbf{r} = (x, y, 0)$ experiences the “electric” vector potential [9, 14, 49] $\mathbf{A}_m(\mathbf{r}) = \mathbf{E}(\mathbf{r}) \times \mathbf{e}_z/c = \mathcal{E}/c(0, x, 0)$. The decoupled Hamiltonian for each magnon ($\sigma \pm 1$) is represented as [9]

$$\mathcal{H}_\sigma = \frac{1}{2m} \left(\hat{\mathbf{p}} + \sigma \frac{g\mu_B}{c} \mathbf{A}_m \right)^2 + \Delta, \quad (1)$$

where $\hat{\mathbf{p}} = (p_x, p_y, 0)$ is the momentum operator, m is the effective mass of magnons, Δ is the magnon gap induced by easy-axis spin anisotropy. See Ref. [9] for the specific expression of m and Δ in terms of the spin language. The total Hamiltonian of the system is given by $\sum_\sigma \mathcal{H}_\sigma$, which respects the TRS effectively in the low-energy regime. The σ -dependence stems from the opposite magnetic dipole moments $\sigma g\mu_B \mathbf{e}_z$ of up and down magnons associated with the Néel order in insulating AFs. This σ -dependence is the key ingredient [10–12] for qualitatively new phenomena in AFs which are not found in FMs [14] such as the violation of the magnonic Wiedemann-Franz (WF) law for Hall transport [9, 14] and the generation of helical edge magnon states. Experiencing the AC vector potential \mathbf{A}_m with $\nabla \times \mathbf{A}_m = (\mathcal{E}/c)\mathbf{e}_z$, magnons of opposite spins form the same Landau levels [9] and performs cyclotron motions with the same frequency $\omega_c = (g\mu_B/mc^2)\mathcal{E}$ and with the same electric length $l_\mathcal{E} \equiv \sqrt{\hbar c^2/g\mu_B \mathcal{E}}$, but in the opposite direction, leading to the helical edge magnon state [59]. Note that the TRS as well as the total spin conservation along the z axis protect the topological phase and helical edge states against nonmagnetic impurities. The key ingredient for the generation of topological edge states is the cyclotron motion in the bulk of the system where up and down magnons are decoupled.

It has been established theoretically that magnonic TIs are realized in the gradient dc electric field. However, whether those states remain intact or not in nonequilibrium, in other words, whether those topological properties are robust against time-dependent perturbation, is still an open issue and the scope of this paper.

III. MAGNON MOTION IN LASER

Applying the laser with a frequency Ω (a period $T = 2\pi/\Omega$) to the insulating AF described by Eq. (1), magnons of opposite spins ($\sigma = \pm 1$) subjected to a periodic electric field $\mathbf{E}(t) = \mathbf{E}(t+T)$ acquire the AC vector potential [13, 14, 49],

$$\mathbf{A}_m(t) = \mathbf{A}_m(t+T), \quad (2)$$

and the Hamiltonian Eq. (1) also becomes time-periodic $\mathcal{H}_\sigma(t) = \mathcal{H}_\sigma(t+T)$. The decoupled Hamiltonian for each magnon ($\sigma = \pm 1$) is specifically written as

$$\mathcal{H}_\sigma(t) = \frac{1}{2m} \left(\hat{\mathbf{p}} + \sigma \frac{g\mu_B}{c} \mathbf{A}_m(t) \right)^2 + \Delta. \quad (3)$$

and the total Hamiltonian of the system is given as $\sum_\sigma \mathcal{H}_\sigma(t)$. Assuming that the system experiences a time-evolution away from the adiabatic limit with the application of high frequency laser $\Omega \gg \omega_c$, the magnon motion is described by the effective Floquet Hamiltonian [31] of Eq. (3), which is represented as $\mathcal{H}_{\text{eff}} = \sum_{n=0}^{\infty} \mathcal{H}_{\text{eff}}^{(n)}$, where the effects of the laser are taken into account perturbatively ($1/\Omega^n$) via each component $\mathcal{H}_{\text{eff}}^{(n)}$ of the high frequency expansion (see Appendix for details).

We remark that though the magnetic field is accompanied by the laser electric field, it does not couple to the orbital motion of magnons, i.e., the linear momentum of magnons but enters the magnon energy directly through the Zeeman coupling without affecting orbital motion. After time-averaging, the effect of the time-varying magnetic field on the magnon energy can be captured by renormalizing the energy gap of magnons, and up and down magnons are still degenerate due to the easy-axis spin anisotropy and the resultant magnon energy gap [60]. On the contrary, an electric field affects the orbital motion of magnons via AC effects and thereby can induce the finite Berry phases for magnons as studied in Refs. [9, 14]. Thus we study the effects of the coupling of an ac electric field of laser to orbital motion of magnons on the magnon bands, looking for possible laser-induced topological phases of magnons. In this paper, our consideration is restricted to the magnon dynamics in the high frequency region $\Omega \gg \omega_c$, where the Floquet Hamiltonian [31] of Eq. (3) can be analyzed through the high-frequency expansion.

A. Linearly polarized laser

First let us consider the case of linearly polarized laser providing the electric field $\mathbf{E}(t) = \mathcal{E}(-x\cos(\Omega t), 0, 0)$. This gives rise to the periodic AC vector potential

$$\mathbf{A}_m(t) = \frac{\mathcal{E}}{c} (0, x\cos(\Omega t), 0), \quad (4)$$

which is time-reversal invariant $\mathbf{A}_m(t) = \mathbf{A}_m(-t)$, and the time averaged value is zero $\bar{\mathbf{A}}_m(t) = 0$. After the high frequency expansion up to $\mathcal{O}(1/\Omega^2)$, we obtain the effective Floquet Hamiltonian as $\mathcal{H}_{\text{eff}} = \mathcal{H}_{\text{eff}}^{(0)} + \mathcal{H}_{\text{eff}}^{(2)}$ (see Appendix for details), where

$$\begin{aligned} \mathcal{H}_{\text{eff}}^{(0)} &= \frac{1}{2m} \left[p_x^2 + p_y^2 + \frac{1}{2} \left(\frac{g\mu_B}{c} \right)^2 \left(\frac{\mathcal{E}}{c} \right)^2 x^2 \right] + \Delta, \\ \mathcal{H}_{\text{eff}}^{(2)} &= \left(\frac{1}{2m} \right)^3 \frac{1}{\Omega^2} \left[2 \left(\frac{g\mu_B}{c} \right)^2 \left(\frac{\mathcal{E}}{c} \right)^2 p_y^2 \right. \\ &\quad \left. + \frac{1}{8} \left(\frac{g\mu_B}{c} \right)^4 \left(\frac{\mathcal{E}}{c} \right)^4 x^2 \right]. \end{aligned} \quad (5)$$

The cancellation of the $\mathcal{H}_{\text{eff}}^{(1)}$ term reflects the time-reversal invariance $\mathbf{A}_m(t) = \mathbf{A}_m(-t)$. From Eq. (5), we find that the effective magnon mass is renormalized as for the motion along the y direction and the confinement by the harmonic potential happens along the x direction, and both effects are irrelevant with topological properties of magnons. Since there are no terms coupling momentum and spatial coordinates such as $p_y x$ and $p_x y$ which play the role of the Lorentz force [61] for magnons, the Landau energy level [9, 14] is not formed and magnons do not perform the cyclotron motion, leading to the absence of any magnon edge states in the high frequency region. Therefore the linearly polarized laser Eq. (4) does not bring any topological properties to magnon transport in the insulating AFs; the absence of any edge magnon states and the topologically trivial bulk without any magnon Hall effects [9, 14, 49].

B. Linearly polarized laser with nonzero time-averaged field

In this section we consider another type of linearly polarized laser $\mathbf{E}(t) = \mathcal{E}(-x\cos^2(\Omega t), 0, 0)$. The resulting periodic AC vector potential is given by

$$\mathbf{A}_m(t) = \frac{\mathcal{E}}{c} (0, x\cos^2(\Omega t), 0), \quad (6)$$

being time-reversal invariant $\mathbf{A}_m(t) = \mathbf{A}_m(-t)$, whereas in contrast to the case of Sec. III A the time averaged value becomes nonzero $\bar{A}_m^y(t) = (\mathcal{E}/2c)x$. After the high frequency expansion ($\Omega \gg \omega_c$), an effective Floquet Hamiltonian $\mathcal{H}_{\text{eff}} = \mathcal{H}_{\text{eff}}^{(0)} + \mathcal{H}_{\text{eff}}^{(2)}$ up to $\mathcal{O}(1/\Omega^2)$ is derived as (see Appendix for details),

$$\mathcal{H}_{\text{eff}} = \frac{1}{2m} \left[p_x^2 + (1+t_0) \left(p_y + \sigma \frac{g\mu_B}{c} \frac{\mathcal{E}_{\text{eff}}}{c} x \right)^2 \right] + \Delta, \quad (7)$$

where

$$\mathcal{E}_{\text{eff}} = \frac{1 + 2t_0}{1 + t_0} \frac{\mathcal{E}}{2} \quad (8)$$

is the effective electric field gradient and $t_0 = (1/32)(\omega_c/\Omega)^2 \propto 1/\Omega^2$. Here the harmonic potential term is dropped since it is irrelevant to topological properties of magnons. Due to the emergence of the effective electric field gradient \mathcal{E}_{eff} , magnons of opposite spins ($\sigma = \pm 1$) form the same Landau energy level and perform the cyclotron motion [9, 14] with the same frequency and the same electric length but in the opposite direction depending on σ as is seen from Eq. (7), which leads to helical edge magnon states.

Note that the total spin conservation and the TRS still holds in the present setup. These symmetries protect the topological phase and helical edge states against nonmagnetic impurities [62].

C. Circularly polarized laser

Next we move on to the case of circularly polarized laser [17, 63, 64]. The laser electric field is $\mathbf{E}(t) = \mathcal{E}(-x\cos(\Omega t), \eta x\sin(\Omega t), 0)$, where $\eta = 1(-1)$ is the index to represent the left (right) circular polarization. Then the periodic AC vector potential becomes

$$\mathbf{A}_m(t) = \frac{\mathcal{E}}{c}(\eta x\sin(\Omega t), x\cos(\Omega t), 0), \quad (9)$$

where the time averaged value vanishes $\bar{\mathbf{A}}_m(t) = 0$ as is the case of Sec. III A, though the time-reversal invariance is violated by the circularly polarized laser $\mathbf{E}(t) \neq \mathbf{E}(-t)$ and $\mathbf{A}_m(t) \neq \mathbf{A}_m(-t)$ [24–26] in contrast to the case of Secs. III A and III B. Again we obtain an effective Floquet Hamiltonian up to $\mathcal{O}(1/\Omega)$ using the high frequency expansion ($\Omega \gg \omega_c$) as $\mathcal{H}_{\text{eff}} = \mathcal{H}_{\text{eff}}^{(0)} + \mathcal{H}_{\text{eff}}^{(1)}$ (see Appendix for details), where

$$\mathcal{H}_{\text{eff}}^{(0)} = \frac{1}{2m} \left[p_x^2 + p_y^2 + \left(\frac{g\mu_B}{c} \right)^2 \left(\frac{\mathcal{E}}{c} \right)^2 x^2 \right] + \Delta, \quad (10a)$$

$$\mathcal{H}_{\text{eff}}^{(1)} = -\eta \frac{\omega_c}{2\Omega} \omega_c p_y x. \quad (10b)$$

After dropping the harmonic potential term for readability due to its irrelevance with topological properties of magnons, the Hamiltonian is recast into

$$\mathcal{H}_{\text{eff}} = \frac{1}{2m} \left[p_x^2 + \left(p_y - \eta \frac{g\mu_B}{c} \frac{\mathcal{E}_{\text{eff}}}{c} x \right)^2 \right] + \Delta, \quad (11a)$$

$$\mathcal{E}_{\text{eff}} = \frac{\omega_c}{2\Omega} \mathcal{E} \propto \frac{1}{\Omega}. \quad (11b)$$

Contrary to Secs. III A and III B, since the circularly polarized laser $\mathbf{E}(t) \neq \mathbf{E}(-t)$ breaks the TRS ($\mathbf{A}_m(t) \neq \mathbf{A}_m(-t)$), the leading correction does not vanish $\mathcal{H}_{\text{eff}}^{(1)} \neq 0$ and brings the term proportional to $p_y x$ [Eq. (10b)] that works as a Lorentz force for magnons [9, 14, 49],

namely, the laser-induced Lorentz force proportional to $1/\Omega$. Note that the force does not depend on the index $\sigma = \pm 1$ for up and down magnons, while it depends on the index $\eta = 1(-1)$ for the left (right) circular polarization of the laser. Therefore both up and down magnons perform the cyclotron motion in the same direction depending on the sign η , differently from the case of the linearly polarized laser in Sec. III B. In other words, the direction of the cyclotron motion can be controlled by tuning the chirality of the circularly polarized laser.

To conclude, in the circularly polarized laser magnons acquire the laser-induced effective electric field gradient $\mathcal{E}_{\text{eff}} \propto 1/\Omega$. Thereby forming the same Landau energy level, magnons of opposite spins ($\sigma = \pm 1$) perform the cyclotron motion along the same direction, leading to the chiral edge magnon states. The direction of the cyclotron motion and that of the resulting chiral edge magnons can be controlled by changing the chirality of the circularly polarized laser between the left-circular or the right-circular polarization ($\eta = \pm 1$) as can be seen from Eqs. (11a) and (11b), which are the main results of this paper. The schematic figure of the present setup and induced chiral magnon edge modes is shown in Fig. 1.

Since the effective gradient electric field [Eq. (11b)] induced by circularly polarized laser vanishes in the high frequency limit $\Omega \rightarrow \infty$, it is interpreted as an ‘emergent’ field having an intrinsically nonequilibrium nature away from the adiabatic limit $\Omega \rightarrow 0$.

D. Laser-driven magnon and symmetry

In the high frequency regime $\Omega \gg \omega_c$ the linearly polarized laser [Eq. (6)] can induce the helical edge magnon states, while the circularly polarized laser [Eq. (9)] can generate the chiral edge magnon states whose direction can be controlled by changing the chirality of the laser, i.e., depending on the index $\eta = 1(-1)$ for the left (right) circular [Eq. (11a)]. Those insulating AFs in laser become topologically nontrivial. Thus depending on the form of the laser, e.g., polarized linearly or circularly, the details of the edges states (i.e., chiral or helical) in the topological AFs vary from system to system. This indicates that by tuning the laser, we can control and design topological properties of antiferromagnetic magnonic systems.

We remark that since $\mathbf{A}_m(t) = \mathbf{A}_m(-t)$ for the linearly polarized laser, those systems described by the Hamiltonian $\mathcal{H}_\sigma(t)$ [Eq. (3)] and the ones by the effective Floquet Hamiltonian $\mathcal{H}_{\text{eff}} = \mathcal{H}_{\text{eff}}^{(0)} + \mathcal{H}_{\text{eff}}^{(2)}$ possess the TRS. The TRS of the system can be seen by the transformation $\mathbf{p} \rightarrow -\mathbf{p}$ and $\sigma \rightarrow -\sigma$. On the other hand, since $\mathbf{A}_m(t) \neq \mathbf{A}_m(-t)$ for the circularly polarized laser, the TRS is broken in the system described by the Hamiltonian $\mathcal{H}_\sigma(t)$ and in the one by the effective Floquet Hamiltonian $\mathcal{H}_{\text{eff}} = \mathcal{H}_{\text{eff}}^{(0)} + \mathcal{H}_{\text{eff}}^{(1)}$ [Eq. (11a)]. This TRS breaking stems from the chirality dependence $\eta = \pm 1$. Those results can be interpreted from the general prop-

TABLE I: High frequency laser-induced magnon motion and the thermomagnetic properties of magnon Hall transport in the insulating AF [Eq. (3)].

Laser of high frequency $\Omega \gg \omega_c$	Linearly polarized laser: Sec. III A	Linearly polarized laser: Sec. III B	Circularly polarized laser: Sec. III C
	$\mathbf{A}_m(t) = \mathbf{A}_m(-t)$ $\bar{\mathbf{A}}_m(t) = 0$	$\mathbf{A}_m(t) = \mathbf{A}_m(-t)$ $ \bar{\mathbf{A}}_m(t) = (\mathcal{E}/2c)x$	$\mathbf{A}_m(t) \neq \mathbf{A}_m(-t)$ $\bar{\mathbf{A}}_m(t) = 0$
\mathcal{H}_{eff}	σ -independent	σ -dependent	σ -independent η -dependent
\mathcal{E}_{eff}	0	$[(1 + 2t_0)/(1 + t_0)](\mathcal{E}/2)$	$(\omega_c/2\Omega)\mathcal{E}$
Topological properties	–	✓	✓
Cyclotron motion of each mode	–	In the opposite direction	In the same direction
Edge states	–	Helical edge states	Chiral edge states
Magnon thermal Hall effect	–	–	✓
Magnon spin Nernst effect	–	✓	–
Magnonic WF law [14]	No Hall effects	–	✓

erties of the Floquet formalism [31]. When the Hamiltonian $\mathcal{H}(t) = \sum_{m \in \mathbb{Z}} H_m e^{im\Omega t}$ possesses the TRS $\mathcal{H}(t) = \mathcal{H}(-t)$, $[H_m, H_{-m}]$ becomes zero due to $H_m = H_{-m}$. Thus the $1/\Omega$ order term of the effective Floquet Hamiltonian $\mathcal{H}_{\text{eff}}^{(1)} = (\hbar\Omega)^{-1} \sum_{m=1}^{\infty} [H_m, H_{-m}]/m$ vanishes. In contrast, when the TRS is broken, the $\mathcal{H}_{\text{eff}}^{(1)}$ term [Eq. (10b)] can be nonzero.

IV. HALL TRANSPORT WITH THE APPLICATION OF LASER

In this section, we discuss the laser-induced thermomagnetic properties of Hall transport in the topological AFs. Within the linear response regime, the spin and heat Hall current densities for each mode ($\sigma = \pm 1$) in the topological AFs subjected to an effective magnetic field gradient (i.e., a gradient of nonequilibrium magnon chemical potential [65]) and a temperature gradient are described by the Onsager matrix of Eq. (31) in Ref. [9]. Within the almost flat band approximation [9, 14, 66, 67], the Onsager coefficients become characterized by the topological invariant (i.e., Chern integer) that edge states bring about.

Since the linearly polarized laser [Eq. (6)] can induce helical edge magnon states, the total Chern number vanishes, while the \mathbb{Z}_2 topological invariant becomes nonzero [9]. Therefore the diagonal elements of the Onsager matrix vanishes, whereas the off-diagonal elements becomes nonzero. This leads to the generation of the magnonic spin Nernst effect, while the vanishment of the magnonic thermal Hall effect. The vanishment of the magnonic spin Hall conductance $G_{\text{AF}}^{yx} = 0$ and the thermal Hall conductance $K_{\text{AF}}^{yx} = 0$ in the AFs indicate that the thermomagnetic ratio $K_{\text{AF}}^{yx}/G_{\text{AF}}^{yx}$ becomes ill-defined due to $G_{\text{AF}}^{yx} = 0$ and that the WF law [14, 28, 68] characterized by the liner-in- T behavior at low temperature becomes violated due to $K_{\text{AF}}^{yx} = 0$ [9].

On the other hand, since the circularly polarized laser [Eq. (9)] can induce chiral edge magnon states [14] the \mathbb{Z}_2 topological invariant [9] vanishes, while the total Chern number becomes nonzero. Therefore the diagonal elements of the Onsager matrix [9] becomes nonzero, whereas the off-diagonal elements vanishes. This leads to the generation of the magnonic thermal Hall effect, while the vanishment of the magnonic spin Nernst effect. The direction of the thermal Hall current can be controlled by switching the chirality of the laser between the left-circular and right-circular polarization ($\eta = \pm 1$) [Eq. (11a)] as shown in Fig. 1. The thermomagnetic ratio satisfies the magnonic WF law [14] at low temperature [27],

$$\frac{K_{\text{AF}}^{yx}}{G_{\text{AF}}^{yx}} \Rightarrow \left(\frac{k_B}{g\mu_B}\right)^2 T, \quad (12)$$

as the topological FM [14] does satisfy. Note that the thermal Hall effect of magnons has been observed in Ref. [69] and the measurement of a magnonic spin conductance has been reported in Ref. [70] where the gradient of a nonequilibrium magnonic spin chemical potential [65, 71–75] plays the role of an effective magnetic field gradient. Thereby we expect that the magnonic WF law [9, 14, 28] can be experimentally confirmed [55, 69, 70, 76–85].

To conclude, depending on the form of laser such as linear or circular polarization, the thermomagnetic properties of Hall transport (e.g., the magnonic WF law) in insulating AFs vary from system to system. This indicates that by tuning the laser, we can control and design thermomagnetic Hall transport properties in antiferromagnetic magnonic systems. Those results for the laser-induced magnon motion and Hall transport properties are summarized in Table I.

V. ESTIMATE FOR EXPERIMENTS

The development of laser techniques [86–88] in quantum optics [89] is remarkably rapid. The advanced laser technologies such as optical tweezers [90], plasmonics [86, 87], near-field [87], and metamaterials [91] enable us to realize the various profile of electric and magnetic fields including an ac electric field gradient we considered in this work.

The thermal Hall effect of magnons has been observed in Ref. [69] and experimental evidence for the magnonic spin Nernst effect has been reported in Ref. [80]. Therefore making use of those measurement techniques, our theoretical predictions (Table I), i.e., laser-induced magnonic topological phases, can be experimentally confirmed by measuring Hall currents. As seen in Sec. IV, the linearly polarized laser can generate helical edge magnon states and induce the magnonic spin Nernst effect, while the circularly polarized laser can generate chiral edge magnon states and induce the magnonic thermal Hall effect (Table I). Thereby measuring Hall currents instead of directly observing edge magnon states [92], our theoretical predictions can be experimentally confirmed [93].

We estimate the experimental feasibility with taking Cr_2O_3 [94, 95] for example following Ref. [9]. This material has the spin quantum number $S = 3/2$, g -factor $g = 2$, the lattice constant $a = 0.5$ nm, the easy-axis anisotropy $\mathcal{K} = 0.03$ meV, and the antiferromagnetic nearest-neighbor spin exchange interaction $J = 15$ meV. The magnon gap arising from the easy-axis spin anisotropy amounts to $\Delta = 4$ meV and the frequency of cyclotron motions becomes $\omega_c = \mathcal{O}(1)$ GHz. Thereby using a picosecond laser [96] $\Omega = \mathcal{O}(1)$ THz and the experimental scheme proposed in Refs. [9, 14], we expect that the laser-induced magnonic topological phases can be realized experimentally in the low temperature regime [27, 97].

Lastly, we comment on the heating effect by laser application. In this paper, we focus on the magnetic insulators with large electronic band gap. Hence electric excitations by the laser electric field are negligible and consequently, the heating through the electron-phonon coupling (e.g., Joule heating) is negligibly small. Thus we only have to consider the heating problem of the isolated quantum system. From Ref. [98], the energy-absorption rate P of the isolated quantum system subjected to periodic driving at the frequency Ω is bounded as $P \leq \hbar\omega_c^2 \exp(-\Omega/\omega_c)$. It is exponentially small in the high frequency regime we considered above. The estimation is given as $\Omega/\omega_c \sim 10^3$ with the parameters $\omega_c = \mathcal{O}(1)$ GHz and $\Omega = \mathcal{O}(1)$ THz. Therefore, we conclude that heating effects are irrelevant in our systems.

VI. DISCUSSION

Before concluding, we make further discussions on several points of this paper and the future problems. First, the mechanism of our laser-induced magnonic topological phases discussed in Sec. III B is different [99] from that of the so-called Floquet TIs [100, 101] in the sense that we do not employ Dirac materials [17, 63, 64] with a relativistic spectrum (i.e., a linear dispersion) or ac field-driven resonance across the band gap [20, 21]. We remark that Dirac magnons having a linear dispersion are available on two-dimensional honeycomb lattices [102]. In Ref. [14], we have studied those Dirac magnons in the AC effect. The correspondence between Dirac magnons in the AC effect and Dirac electrons in the AB effect [63, 64] is straightforward. For example, by simply replacing the Fermi velocity, electric charge, and the AB vector potential [56] with the magnon velocity, $g\mu_B$, and \mathbf{A}_m , respectively, one can map the equation for Dirac electrons in the AB effect to that for Dirac magnons in the AC effect. Compare Eq. (1) of Ref. [63] with Eq. (D1) of Ref. [14]. Therefore by applying this mapping to Floquet TIs established in Dirac electron systems [63, 64], the magnonic analog of the Floquet TIs can be derived theoretically [103–106]. Moreover, while it is outside the scope of this work since we focus on the magnon dynamics away from the adiabatic limit $\Omega \gg \omega_c$, the laser-induced resonance across the Landau energy gap of magnons is expected to be generated, in the same way as the ac field-driven resonance across the band gap [20, 21], by tuning the laser frequency to the cyclotron frequency of magnons $\Omega \approx \omega_c$, which we leave for the further study [99].

Second, we comment on the effect of the Dzyaloshinskii-Moriya interaction (DMI) [107–109]. When the inversion symmetry is broken, a time-independent DMI indeed can exist and work as a vector potential [110] for magnons in the similar way as the AC phase \mathbf{A}_m induced by electric field gradient. However, a spatially uniform DMI does not give rise to any emergent electromagnetic field that acts as the Lorentz force on magnons and thus should not change the qualitative behavior of magnons obtained in our work. We thus conclude that our results, topological phenomena associated with the Landau quantization of Floquet magnons, qualitatively remain unchanged even in the presence of such DMI. Those topological phenomena are stable even with the Rashba-like splitting of the bands provoked by the DMI, which retains TRS. Since the possible type of DMI strongly depends on the details of the system, e.g., the lattice geometry and the magnetic point group, the comprehensive study on the effects caused by DMI is beyond the scope of the present paper. The effect from the interplay of DMI and magnon chirality in AFs has been investigated including the optical excitations such as magnon photocurrents [10–12]. Those results are helpful for our future study.

Third, a general treatment of nonequilibrium-driven topological phases in AFs beyond our theoretical frame-

work [111] remains an open problem such as disorder effects due to magnetic impurities or the effects of hybridization of spin-up and spin-down magnons due to the symmetry/conservation breaking terms. While we treat the steady state in terms of the Floquet theory in this paper, considering the transient dynamics, thermalization, and open systems [98, 112] in the laser application is an interesting future problem.

Last, applying a laser to magnets is just one of the ways to drive magnets into nonequilibrium. We envision that subjecting magnetic systems to various types of nonequilibrium driving, e.g., time-varying thermal environment or charge/heat currents, can be versatile means to realize novel topological phases in magnetic systems.

VII. SUMMARY

Let us summarize our results. Assuming that the total spin along the z axis is conserved, we have established the laser control of magnonic topological phases in the AF by making use of the AC effect on magnons in laser. Using the Floquet formalism, we have found in the high frequency regime that the linearly polarized laser can generate helical edge magnon states and induce the magnonic spin Nernst effect, while the circularly polarized laser can generate chiral edge magnon states and induce the magnonic thermal Hall effect. We have thus provided a handle to control and design topological properties of the insulating AF. Our result for controlling magnonic topological phases by laser provides a new direction for development of magnonics, and will serve as a bridge between two research areas, magnonics and quantum optics.

Acknowledgments

We acknowledge support by the Leading Initiative for Excellent Young Researchers, MEXT, Japan (KN), the startup fund at the University of Missouri (SKK), the Swiss National Science Foundation under Division II (ST) and ImPact project (No. 2015-PM12-05-01) from the Japan Science and Technology Agency (ST). We (KN) would like to thank K. Usami for useful feedback on the laser experiment and D. Loss for fruitful discussions about the significance of this work. KN is grateful to the hospitality of the T. Giamarchi-group (U. Geneva) during his stay where a part of this work was carried out.

Appendix: Floquet formalism

In this Appendix, for completeness, we provide details of the straightforward calculation of the effective Floquet Hamiltonian. For a general framework of the Floquet formalism, see the review article Ref. [31].

1. Floquet Hamiltonian and high frequency expansion

First let us explain the derivation of the Floquet effective model and the high frequency expansion. This strategy is applicable to general time-periodic systems. Assume that the Hamiltonian has a temporal periodicity $\mathcal{H}(t) = \mathcal{H}(t+T)$, where T is the period. We can perform the Fourier transform on the time-dependent Hamiltonian

$$\mathcal{H}(t) = \sum_{m \in \mathbb{Z}} H_m e^{im\Omega t}, \quad (\text{A.1})$$

where $\Omega = 2\pi/T$. Although it is a difficult problem to obtain the exact Floquet effective Hamiltonian

$$\mathcal{H}_{\text{eff}} \equiv \frac{i}{T} \ln \mathcal{T} \exp \left[-i \int_0^T \mathcal{H}(t) dt \right],$$

where \mathcal{T} is the time-ordering, we can calculate it for the high frequency regime $\Omega \gg \omega_c$ in the perturbation way using the high frequency expansion [19, 31],

$$\mathcal{H}_{\text{eff}} = \sum_{n=0}^{\infty} \mathcal{H}_{\text{eff}}^{(n)}. \quad (\text{A.2})$$

Here $\mathcal{H}_{\text{eff}}^{(n)}$ is the $1/\Omega^n$ order term. We give the explicit formula up to $\mathcal{O}(1/\Omega^2)$,

$$\mathcal{H}_{\text{eff}}^{(0)} = H_0, \quad (\text{A.3})$$

$$\mathcal{H}_{\text{eff}}^{(1)} = \frac{1}{\hbar\Omega} \sum_{m=1}^{\infty} \frac{[H_m, H_{-m}]}{m}, \quad (\text{A.4})$$

$$\begin{aligned} \mathcal{H}_{\text{eff}}^{(2)} = & \frac{1}{(\hbar\Omega)^2} \sum_{m \neq 0} \left(\frac{[H_{-m}, [H_0, H_m]]}{2m^2} \right. \\ & \left. + \sum_{m' \neq 0, m' \neq m} \frac{[H_{-m'}, [H_{m'-m}, H_m]]}{3mm'} \right). \end{aligned} \quad (\text{A.5})$$

The $1/\Omega$ order term Eq. (A.4) vanishes when the Hamiltonian has time-reversal invariance $\mathcal{H}(t) = \mathcal{H}(-t)$ since $[H_m, H_{-m}] = 0$.

2. Application to the insulating AF

Next we apply the Floquet theory described in Sec. 1 to the insulating AF with the laser application.

Section III A in the main text: Each Fourier component H_m [Eq. (A.1)] for the periodic AC vector potential of $\mathbf{A}_m(t) = (\mathcal{E}/c)(0, x \cos(\Omega t), 0)$ becomes

$$H_0 = \frac{1}{2m} \left[p_x^2 + p_y^2 + \frac{1}{2} \left(\frac{g\mu_B}{c} \right)^2 \left(\frac{\mathcal{E}}{c} \right)^2 x^2 \right] + \Delta,$$

$$H_1 = H_{-1} = \sigma \frac{1}{2m} \frac{g\mu_B}{c} \frac{\mathcal{E}}{c} p_y x,$$

$$H_2 = H_{-2} = \frac{1}{4} \frac{1}{2m} \left(\frac{g\mu_B}{c} \right)^2 \left(\frac{\mathcal{E}}{c} \right)^2 x^2,$$

where $[H_1, H_{-1}] = [H_2, H_{-2}] = 0$ due to $\mathbf{A}_m(t) = \mathbf{A}_m(-t)$. Using the high frequency expansion [Eqs. (A.3)-(A.5)], we obtain the effective Floquet Hamiltonian $\mathcal{H}_{\text{eff}}^{(n)}$ [Eq. (A.2)] in the main text.

Section III B in the main text: Each Fourier component H_m [Eq. (A.1)] for the periodic AC vector potential of $\mathbf{A}_m(t) = (\mathcal{E}/c)(0, x\cos^2(\Omega t), 0)$ becomes

$$\begin{aligned} H_0 &= \frac{1}{2m} \left[p_x^2 + p_y^2 + \sigma \frac{g\mu_B}{c} \frac{\mathcal{E}}{c} p_y x + \frac{3}{8} \left(\frac{g\mu_B}{c} \right)^2 \left(\frac{\mathcal{E}}{c} \right)^2 x^2 \right] + \Delta, \\ H_2 &= H_{-2} = \frac{1}{2m} \left[\sigma \frac{1}{2} \frac{g\mu_B}{c} \frac{\mathcal{E}}{c} p_y x + \frac{1}{4} \left(\frac{g\mu_B}{c} \right)^2 \left(\frac{\mathcal{E}}{c} \right)^2 x^2 \right], \\ H_4 &= H_{-4} = \frac{1}{16} \frac{1}{2m} \left(\frac{g\mu_B}{c} \right)^2 \left(\frac{\mathcal{E}}{c} \right)^2 x^2, \end{aligned}$$

where $[H_2, H_{-2}] = [H_4, H_{-4}] = 0$ due to $\mathbf{A}_m(t) = \mathbf{A}_m(-t)$. The high frequency expansion for $\Omega \gg \omega_c$ [Eqs. (A.3)-(A.5)] provides the effective Floquet Hamiltonian up to $\mathcal{O}(1/\Omega^2)$ as $\mathcal{H}_{\text{eff}} = \mathcal{H}_{\text{eff}}^{(0)} + \mathcal{H}_{\text{eff}}^{(2)}$:

$$\begin{aligned} \mathcal{H}_{\text{eff}}^{(0)} &= \frac{1}{2m} \left[p_x^2 + \left(p_y + \sigma \frac{g\mu_B}{c} \frac{\mathcal{E}/2}{c} x \right)^2 \right] + \frac{\mathcal{F}_0}{3} x^2 + \Delta, \\ \mathcal{H}_{\text{eff}}^{(2)} &= \frac{t_0}{2m} \left(p_y + \sigma \frac{g\mu_B}{c} \frac{\mathcal{E}}{c} x \right)^2 + \mathcal{F}_2 x^2, \end{aligned}$$

where $\mathcal{F}_0 = (3/8)(g\mu_B/c)^2(\mathcal{E}/c)^2/2m$, $\mathcal{F}_2 = (1/2\Omega^2)(1/16)^2(1/2m)^3(g\mu_B/c)^4(\mathcal{E}/c)^4$, and $t_0 = (1/32)(\omega_c/\Omega)^2 \propto 1/\Omega^2$. It is rewritten as

$$\begin{aligned} \mathcal{H}_{\text{eff}} &= \frac{1}{2m} \left[p_x^2 + (1+t_0) \left(p_y + \sigma \frac{g\mu_B}{c} \frac{\mathcal{E}_{\text{eff}}}{c} x \right)^2 \right] \\ &\quad + \mathcal{F} x^2 + \Delta, \end{aligned} \quad (\text{A.6})$$

where $\mathcal{F} = \mathcal{F}_0 + \mathcal{F}_2 + \mathcal{F}_t - \mathcal{F}_3$, $\mathcal{F}_t = (g\mu_B/c)^2(\mathcal{E}/c)^2 t_0/2m$, $\mathcal{F}_3 = [(1+2t_0)^2/(1+t_0)](g\mu_B/c)^2(\mathcal{E}/c)^2/8m$. The effective electric field gradient in Eq. (A.6) is given by $\mathcal{E}_{\text{eff}} = [(1+2t_0)/(1+t_0)]\mathcal{E}/2$.

Section III C in the main text: Each Fourier component H_m [Eq. (A.1)] for the periodic AC vector potential of $\mathbf{A}_m(t) = (\mathcal{E}/c)(\eta x \sin(\Omega t), x \cos(\Omega t), 0)$ becomes

$$\begin{aligned} H_0 &= \frac{1}{2m} \left[p_x^2 + p_y^2 + \left(\frac{g\mu_B}{c} \right)^2 \left(\frac{\mathcal{E}}{c} \right)^2 x^2 \right] + \Delta, \\ H_1 &= -\frac{\hbar}{4m} \sigma \frac{g\mu_B}{c} \frac{\mathcal{E}}{c} \eta + \frac{1}{2m} \sigma \frac{g\mu_B}{c} \frac{\mathcal{E}}{c} (-i\eta x p_x + x p_y), \\ H_{-1} &= \frac{\hbar}{4m} \sigma \frac{g\mu_B}{c} \frac{\mathcal{E}}{c} \eta + \frac{1}{2m} \sigma \frac{g\mu_B}{c} \frac{\mathcal{E}}{c} (i\eta x p_x + x p_y), \end{aligned}$$

where $[H_1, H_{-1}] \neq 0$ due to $\mathbf{A}_m(t) \neq \mathbf{A}_m(-t)$. Using the high frequency expansion [Eqs. (A.3)-(A.5)], we obtain $\mathcal{H}_{\text{eff}}^{(0)}$ and $\mathcal{H}_{\text{eff}}^{(1)}$ in the main text, and the effective Floquet Hamiltonian $\mathcal{H}_{\text{eff}} = \mathcal{H}_{\text{eff}}^{(0)} + \mathcal{H}_{\text{eff}}^{(1)}$ is rewritten as

$$\begin{aligned} \mathcal{H}_{\text{eff}} &= \frac{1}{2m} \left[p_x^2 + \left(p_y - \eta \frac{g\mu_B}{c} \frac{\mathcal{E}_{\text{eff}}}{c} x \right)^2 \right] + \Delta \\ &\quad + \frac{1}{2m} \left[1 - \left(\frac{\omega_c}{2\Omega} \right)^2 \right] \left(\frac{g\mu_B}{c} \right)^2 \left(\frac{\mathcal{E}}{c} \right)^2 x^2. \end{aligned}$$

-
- [1] A. V. Chumak, V. I. Vasyuchka, A. A. Serga, and B. Hillebrands, *Nat. Phys.* **11**, 453 (2015).
[2] K. Nakata, P. Simon, and D. Loss, *J. Phys. D: Appl. Phys.* **50**, 114004 (2017).
[3] T. Jungwirth, X. Marti, P. Wadley, and J. Wunderlich, *Nat. Nanotech.* **11**, 231 (2016).
[4] E. V. Gomonaya and V. M. Loktev, *Low Temp. Phys.* **40**, 17 (2014).
[5] V. Baltz, A. Manchon, M. Tsoi, T. Moriyama, T. Ono, and Y. Tserkovnyak, *Rev. Mod. Phys.* **90**, 015005 (2018).
[6] S. O. Demokritov, V. E. Demidov, O. Dzyapko, G. A. Melkov, A. A. Serga, B. Hillebrands, and A. N. Slavin, *Nature* **443**, 430 (2006).
[7] R. Shindou, R. Matsumoto, S. Murakami, and J. Ohe, *Phys. Rev. B* **87**, 174427 (2013).
[8] R. Shindou, J. Ohe, R. Matsumoto, S. Murakami, and E. Saitoh, *Phys. Rev. B* **87**, 174402 (2013).
[9] K. Nakata, S. K. Kim, J. Klinovaja, and D. Loss, *Phys. Rev. B* **96**, 224414 (2017).
[10] I. Proskurin, R. L. Stamps, A. S. Ovchinnikov, and J. Kishine, *Phys. Rev. Lett.* **119**, 177202 (2017).
[11] I. Proskurin, A. S. Ovchinnikov, J. Kishine, and R. L. Stamps, *Phys. Rev. B* **98**, 134422 (2018).
[12] M. W. Daniels, R. Cheng, W. Yu, J. Xiao, and D. Xiao, *Phys. Rev. B* **98**, 134450 (2018).
[13] Y. Aharonov and A. Casher, *Phys. Rev. Lett.* **53**, 319 (1984).
[14] K. Nakata, J. Klinovaja, and D. Loss, *Phys. Rev. B* **95**, 125429 (2017).
[15] S. Iwai, M. Ono, A. Maeda, H. Matsuzaki, H. Kishida, H. Okamoto, and Y. Tokura, *Phys. Rev. Lett.* **91**, 057401 (2003).
[16] T. Ishikawa, Y. Sagae, Y. Naitoh, Y. Kawakami, H. Itoh, K. Yamamoto, K. Yakushi, H. Kishida, T. Sasaki, S. Ishihara, et al., *Nat. Comm.* **5**, 5528 (2014).
[17] T. Oka and H. Aoki, *Phys. Rev. B* **79**, 081406(R) (2009).
[18] T. Kitagawa, T. Oka, A. Brataas, L. Fu, and E. Demler, *Phys. Rev. B* **84**, 235108 (2011).
[19] T. Mikami, S. Kitamura, K. Yasuda, N. Tsuji, T. Oka, and H. Aoki, *Phys. Rev. B* **93**, 144307 (2016).
[20] J. Klinovaja, P. Stano, and D. Loss, *Phys. Rev. Lett.* **116**, 176401 (2016).
[21] M. Thakurathi, D. Loss, and J. Klinovaja, *Phys. Rev. B* **95**, 155407 (2017).
[22] A. Kimel, A. Kirilyuk, P. Usachev, R. Pisarev, A. Balbashov, and T. Rasing, *Nature* **435**, 655 (2005).

- [23] A. Kirilyuk, A. V. Kimel, and T. Rasing, *Rev. Mod. Phys.* **82**, 2731 (2010).
- [24] S. Takayoshi, H. Aoki, and T. Oka, *Phys. Rev. B* **90**, 085150 (2014).
- [25] S. Takayoshi, M. Sato, and T. Oka, *Phys. Rev. B* **90**, 214413 (2014).
- [26] M. Sato, S. Takayoshi, and T. Oka, *Phys. Rev. Lett.* **117**, 147202 (2016).
- [27] S. Kosen, R. G. E. Morris, A. F. van Loo, and A. D. Karenowska, *Appl. Phys. Lett.* **112**, 012402 (2018).
- [28] K. Nakata, P. Simon, and D. Loss, *Phys. Rev. B* **92**, 134425 (2015).
- [29] H. Adachi, K. Uchida, E. Saitoh, J. Ohe, S. Takahashi, and S. Maekawa, *Appl. Phys. Lett.* **97**, 252506 (2010).
- [30] N. Prasai, B. A. Trump, G. G. Marcus, A. Akopyan, S. X. Huang, T. M. McQueen, and J. L. Cohn, *Phys. Rev. B* **95**, 224407 (2017).
- [31] M. Bukov, L. D. Alessio, and A. Polkovnikov, *Adv. Phys.* **64**, 139 (2015).
- [32] H. Katsura, N. Nagaosa, and P. A. Lee, *Phys. Rev. Lett.* **104**, 066403 (2010).
- [33] R. Matsumoto and S. Murakami, *Phys. Rev. Lett.* **106**, 197202 (2011).
- [34] R. Matsumoto and S. Murakami, *Phys. Rev. B* **84**, 184406 (2011).
- [35] S. Murakami and A. Okamoto, *J. Phys. Soc. Jpn.* **86**, 011010 (2017).
- [36] Y. Ohnuma, H. Adachi, E. Saitoh, and S. Maekawa, *Phys. Rev. B* **87**, 014423 (2013).
- [37] R. Cheng, S. Okamoto, and D. Xiao, *Phys. Rev. Lett.* **117**, 217202 (2016).
- [38] V. A. Zyuzin and A. A. Kovalev, *Phys. Rev. Lett.* **117**, 217203 (2016).
- [39] F. Bloch, *Z. Physik* **61**, 206 (1930).
- [40] C. Kittel, *Phys. Rev.* **73**, 155 (1948).
- [41] T. Holstein and H. Primakoff, *Phys. Rev.* **58**, 1098 (1940).
- [42] P. W. Anderson, *Phys. Rev.* **86**, 694 (1952).
- [43] R. Kubo, *Phys. Rev.* **87**, 568 (1952).
- [44] M. Z. Hasan and C. L. Kane, *Rev. Mod. Phys.* **82**, 3045 (2010).
- [45] X. L. Qi and S. C. Zhang, *Rev. Mod. Phys.* **83**, 1057 (2011).
- [46] See Ref. [113] for a magnonic TI in insulating ferrimagnets.
- [47] R. Mignani, *J. Phys. A: Math. Gen.* **24**, L421 (1991).
- [48] A. V. Balatsky and B. L. Altshuler, *Phys. Rev. Lett.* **70**, 1678 (1993).
- [49] F. Meier and D. Loss, *Phys. Rev. Lett.* **90**, 167204 (2003).
- [50] K. Nakata, K. A. van Hoogdalem, P. Simon, and D. Loss, *Phys. Rev. B* **90**, 144419 (2014).
- [51] K. Nakata, P. Simon, and D. Loss, *Phys. Rev. B* **92**, 014422 (2015).
- [52] M. Ericsson and E. Sjöqvist, *Phys. Rev. A* **65**, 013607 (2001).
- [53] T. Liu and G. Vignale, *Phys. Rev. Lett.* **106**, 247203 (2011).
- [54] T. Liu and G. Vignale, *J. Appl. Phys.* **111**, 083907 (2012).
- [55] X. Zhang, T. Liu, M. E. Flatte, and H. X. Tang, *Phys. Rev. Lett.* **113**, 037202 (2014).
- [56] Y. Aharonov and D. Bohm, *Phys. Rev.* **115**, 485 (1959).
- [57] D. Loss, P. Goldbart, and A. V. Balatsky, *Phys. Rev. Lett.* **65**, 1655 (1990).
- [58] D. Loss and P. M. Goldbart, *Phys. Rev. B* **45**, 13544 (1992).
- [59] The force acting on magnons in the dc electric field [Eq. (1)] is invariant under a gauge transformation [9] and the gauge invariance is specific to only magnons, i.e. electrically neutral particles.
- [60] The magnon gap due to the easy-axis spin anisotropy amounts to $\Delta = 4$ meV for [94, 95] Cr_2O_3 , see Ref. [9] for details of experiment parameter values. Compared with it, the magnetic energy due to the resulting ac magnetic field from the applied laser (i.e., ac electric field), e.g., picosecond laser [96] $\Omega = \mathcal{O}(1)$ THz, is negligibly small. Furthermore, the magnetic energy can be substantially softened by allowing for a periodic extension of linear electric field gradients [9, 14].
- [61] See Eq. (14) in Ref. [9] for the details of the Lorentz force [49] for magnons in the AC vector potential.
- [62] See Ref. [111] for \mathbb{Z}_2 topological invariant of a general magnon spin Hall system.
- [63] P. M. Perez-Piskunow, G. Usaj, C. A. Balseiro, and L. E. F. F. Torres, *Phys. Rev. B* **89**, 121401(R) (2014).
- [64] G. Usaj, P. M. Perez-Piskunow, L. E. F. F. Torres, and C. A. Balseiro, *Phys. Rev. B* **90**, 115423 (2014).
- [65] C. Du, T. V. der Sar, T. X. Zhou, P. Upadhyaya, F. Casola, H. Zhang, M. C. Onbasli, C. A. Ross, R. L. Walsworth, Y. Tserkovnyak, et al., *Science* **357**, 195 (2017).
- [66] B. Xu, T. Ohtsuki, and R. Shindou, *Phys. Rev. B* **94**, 220403(R) (2016).
- [67] K. A. van Hoogdalem, Y. Tserkovnyak, and D. Loss, *Phys. Rev. B* **87**, 024402 (2013).
- [68] R. Franz and G. Wiedemann, *Annalen der Physik* **165**, 497 (1853).
- [69] Y. Onose, T. Ideue, H. Katsura, Y. Shiomi, N. Nagaosa, and Y. Tokura, *Science* **329**, 297 (2010).
- [70] L. J. Cornelissen, J. Shan, and B. J. van Wees, *Phys. Rev. B* **94**, 180402(R) (2016).
- [71] M. Johnson and R. H. Silsbee, *Phys. Rev. B* **35**, 4959 (1987).
- [72] V. Basso, E. Ferraro, A. Magni, A. Sola, M. Kuepferling, and M. Pasquale, *Phys. Rev. B* **93**, 184421 (2016).
- [73] V. Basso, E. Ferraro, and M. Piazza, *Phys. Rev. B* **94**, 144422 (2016).
- [74] V. Basso, E. Ferraro, and M. Piazza, *Phys. Rev. B* **94**, 179907 (2016).
- [75] L. J. Cornelissen, K. J. H. Peters, G. E. W. Bauer, R. A. Duine, and B. J. van Wees, *Phys. Rev. B* **94**, 014412 (2016).
- [76] E. Saitoh, M. Ueda, H. Miyajima, and G. Tatara, *Appl. Phys. Lett.* **88**, 182509 (2006).
- [77] Y. Kajiwara, K. Harii, S. Takahashi, J. Ohe, K. Uchida, M. Mizuguchi, H. Umezawa, H. Kawai, K. Ando, K. Takanashi, et al., *Nature* **464**, 262 (2010).
- [78] K. Uchida, J. Xiao, H. Adachi, J. Ohe, S. Takahashi, J. Ieda, T. Ota, Y. Kajiwara, H. Umezawa, H. Kawai, et al., *Nat. Mater.* **9**, 894 (2010).
- [79] S. Seki, T. Ideue, M. Kubota, Y. Kozuka, R. Takagi, M. Nakamura, Y. Kaneko, M. Kawasaki, and Y. Tokura, *Phys. Rev. Lett.* **115**, 266601 (2015).
- [80] Y. Shiomi, R. Takashima, and E. Saitoh, *Phys. Rev. B* **96**, 134425 (2017).
- [81] J. Liu, L. J. Cornelissen, J. Shan, T. Kuschel, and B. J. van Wees, *Phys. Rev. B* **95**, 140402(R) (2017).

- [82] K. Tanabe, R. Matsumoto, J. Ohe, S. Murakami, T. Moriyama, D. Chiba, K. Kobayashi, and T. Ono, *Appl. Phys. Express* **7**, 053001 (2014).
- [83] J. Stigloher, M. Decker, H. Körner, K. Tanabe, T. Moriyama, T. Taniguchi, H. Hata, M. Madami, G. Gubbiotti, K. Kobayashi, et al., *Phys. Rev. Lett.* **117**, 037204 (2016).
- [84] K. Tanabe, R. Matsumoto, J. Ohe, S. Murakami, T. Moriyama, D. Chiba, K. Kobayashi, and T. Ono, *Phys. Status Solidi B* **253**, 783 (2016).
- [85] S. O. Demokritov, B. Hillebrands, and A. N. Slavin, *Phys. Rep.* **348**, 441 (2001).
- [86] D. Bossini, V. I. Belotelov, A. K. Zvezdin, A. N. Kalish, and A. V. Kimel, *ACS Photonics* **3**, 1385 (2016).
- [87] M. F. Ciappina, J. A. P.-Hernandez, A. S. Landsman, W. A. Okell, S. Zherebtsov, B. Forg, J. Schotz, L. Seifert, T. Fennel, T. Shaaran, et al., *Rep. Prog. Phys.* **80**, 054401 (2017).
- [88] T. Arikawa, S. Morimoto, and K. Tanaka, *Opt. Express* **25**, 13728 (2017).
- [89] R. J. Glauber, *Phys. Rev.* **130**, 2529 (1963).
- [90] A. Ashkin, *Phys. Rev. Lett.* **24**, 156 (1970).
- [91] Y. Mukai, H. Hirori, T. Yamamoto, H. Kageyama, and K. Tanaka, *Appl. Phys. Lett.* **105**, 022410 (2014).
- [92] We expect that neutron scattering measurements [114, 115] will be one of the promising strategies for the observation of magnon edge states.
- [93] The AC effect in magnetic systems has also been experimentally confirmed in Ref. [55].
- [94] J. O. Artman, J. C. Murphy, and S. Foner, *Phys. Rev.* **138**, A912 (1965).
- [95] Y. Kota and H. Imamura, *Appl. Phys. Express* **10**, 013002 (2017).
- [96] P. L. Liu, R. Yen, N. Bloembergen, and R. T. Hodgson, *Appl. Phys. Lett.* **34**, 864 (1979).
- [97] Note that even a femtosecond laser pulse is now available [116].
- [98] T. Mori, T. Kuwahara, and K. Saito, *Phys. Rev. Lett.* **116**, 120401 (2016).
- [99] D. Loss, private communication (2017).
- [100] J. Cayssol, B. Dora, F. Simon, and R. Moessner, *Phys. Status Solidi RRL* **7**, 101 (2013).
- [101] N. H. Lindner, G. Refael, and V. Galitski, *Nat. Phys.* **7**, 490 (2011).
- [102] J. Fransson, A. M. B.-Schaffer, and A. V. Balatsky, *Phys. Rev. B* **94**, 075401 (2016).
- [103] S. A. Owerre, *J. Phys. Commun.* **1**, 021002 (2017).
- [104] S. A. Owerre, *Ann. Phys. (N. Y.)* **399**, 93 (2018).
- [105] S. A. Owerre, *Sci. Rep.* **8**, 4431 (2018).
- [106] S. A. Owerre, *Sci. Rep.* **8**, 10098 (2018).
- [107] I. Dzyaloshinskii, *J. Phys. Chem. Solids* **4**, 241 (1958).
- [108] T. Moriya, *Phys. Rev.* **120**, 91 (1960).
- [109] T. Moriya, *Phys. Rev. Lett.* **4**, 228 (1960).
- [110] H. Katsura, N. Nagaosa, and A. V. Balatsky, *Phys. Rev. Lett.* **95**, 057205 (2005).
- [111] H. Kondo, Y. Akagi, and H. Katsura, *Phys. Rev. B* **99**, 041110(R) (2019).
- [112] T. Kuwahara, T. Mori, and K. Saito, *Ann. Phys.* **367**, 96 (2016).
- [113] S. K. Kim, K. Nakata, D. Loss, and Y. Tserkovnyak, *Phys. Rev. Lett.* **122**, 057204 (2019).
- [114] M. Mena, R. Perry, T. Perring, M. Le, S. Guerrero, M. Storni, D. Adroja, C. Rüegg, and D. McMorrow, *Phys. Rev. Lett.* **113**, 047202 (2014).
- [115] R. Chisnell, J. S. Helton, D. E. Freedman, D. K. Singh, R. I. Bewley, D. G. Nocera, and Y. S. Lee, *Phys. Rev. Lett.* **115**, 147201 (2015).
- [116] Y. Izawa, Y. Izawa, Y. Setsuhara, M. Hashida, M. Fujita, R. Sasaki, H. Nagai, and M. Yoshida, *Appl. Phys. Lett.* **90**, 044107 (2007).